BBAA VI International Colloquium on:
Bluff Bodies Aerodynamics & Applications
Milano, Italy, July, 20-24 2008

FLOW AROUND WALL-MOUNTED CYLINDERS WITH DIFFERENT GEOMETRIES: EXPERIMENT AND SIMULATION

Stefan Becker, Irfan Ali, and Thomas Uffinger

Institute of Fluid Mechanics
University of Erlangen-Nuremberg, Cauerstr. 4, 91058 Erlangen, Germany
e-mail: sbecker@lstm.uni-erlangen.de

Keywords: LDA-measurements, CFD, turbulence models, instationary flow

1 INTRODUCTION

Studies of flow around simplified ground bound cylinders are a major contribution to understand the fundamental basics of bluff body aerodynamics. Currently interests are also focused on the sound radiated field of such geometries. Cylindrical geometries are present in many engineering applications such as the pantographs of trains, high-rise buildings, car antennas, beams, fences and supports in internal and external flows. Therefore, the flow around cylindrical objects has been the subject of a large number of research activities.

The selected geometries are based on previous investigations of the flow induced sound field. The results show that drag reduction does not correspond automatically with the flow induced sound for the different wall mounted cylinder geometries [1].

To get a better physical understanding about these phenomena very extensive investigations of the basic flow and turbulence field were done by using experimental and numerical methods. Based on the acoustic part of the objective, the work was focused on the instationary flow field and the turbulence quantities. It shows a direct comparison between both methods depends on the different turbulence modeling in the simulations. Necessary accuracy of the simulations with respect to flow induced sound prediction will be discussed.

The setup investigated in this work is shown in Fig. 1. A rigid square cylinder with edge length D is mounted vertically on a flat wall. The cylinder has a constant aspect ratio (L/D) of 6. The flow over a finite-length cylinder is strongly three-dimensional due to the interaction of the tip vortex with the Kármán vortex shedding and the horseshoe vortex. The resulting flow field strongly depends on the aspect ratio and the ratio between cylinder length L and the boundary layer thickness [2], [3], [4]. When the aspect ratio exceeds 5 (smooth geometries), periodic spanwise vortex shedding occurs over almost the whole span except very close to the wall. Additional separation occurs from the top of the cylinder, but the flow region behind the cylinder is dominated from the spanwise vortex shedding. The general flow structure for this case is depicted in Fig. 2.

The nature and the thickness of the boundary layer in relation to the cylinder length influences the flow field. On approaching the cylinder, the boundary layer separates due to the adverse pressure gradient inducing vortices which are being stretched around the cylinder form-

ing a horseshoe vortex. The Strouhal number St related to the spanwise vortex shedding frequency increases with increase in the ratio between cylinder length and boundary layer thickness.

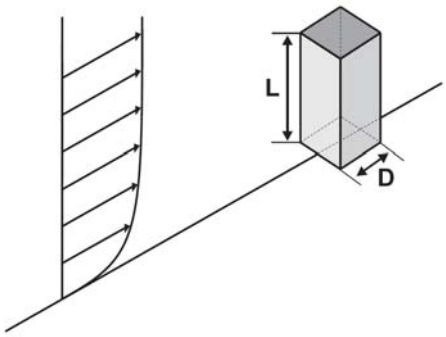

Figure 1: Basic setup: Wall mounted square cylinder in cross-flow

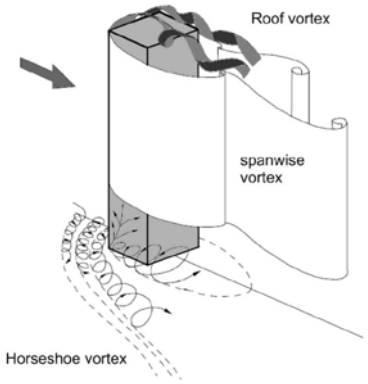

Figure 2: Flow structure behind a square prism with aspect ratio L/D > 5 [3]

Different shapes are used as fore- or afterbodies on the square cylinder and their influence on the flow field is studied. Starting from the basic square cylinder geometries with an additional elliptical forebody (outer dimensions 20 x 30 mm), an elliptical afterbody with the same dimensions and a three-edged wedge (dimensions 20 x 10 mm) are tested. The square cylinder itself has a edge length of D = 20 mm and a length of L = 120 mm.

2 EXPERIMENTAL INVESTIGATIONS

The measurements of the flow field were carried out in the aerodynamic wind tunnel of the institute using a two-component laser Doppler anemometer. Here, the square cylinder is not placed on the floor of the tunnel. Instead, it is mounted in the center of a plate (thickness 12 mm) which is located about 0.5 m above the tunnel floor and extends 1 m in the streamwise direction and 0.6 m in the lateral direction (Fig. 3). At the leading edge of the plate an NACA 0001 profile is attached. Thereby a thiner boundary layer compared with the cylinder length can be obtained. The leading edge of the plate is located 0.5 m downstream of the exit cross-section of the wind tunnel. The aerodynamic wind tunnel is also of closed return type. The nozzle exit cross-section has a width of 1.87 m in the horizontal direction and a height of 1.4 m in the vertical direction (contraction ratio 5:1). The turbulence level of this tunnel is 0.12%.

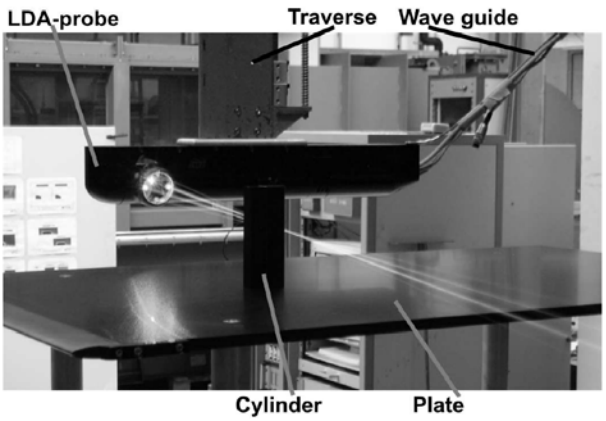

Figure 3: LDA - probe during the measurements

Measurements are carried out at U_0 = 10 m/s and U_0 = 30 m/s, resulting in Reynolds numbers Re_D of $12.5 \cdot 10^4$ and $37.6 \cdot 10^4$ based on the cylinder edge length D. When carrying out measurements at a flow speed of 30 m/s, in both tunnels, a tripping tape is placed near the upstream end of the plate in order to create a well-defined turbulent boundary layer.

The flow field of these selected configurations is investigated via LDA (Fig. 4) illustrates the three-dimensional flow field of the selected test cases. They show a visualization of the flow, the velocity and the turbulent kinetic energy distribution in different planes. The horseshoe vortex system in front of the cylinder caused by the adverse pressure gradient of the stagnation point, the recirculation zone and the wake behind the cylinder are typical flow features of these cases. On the edges of the cylinder side-faces the flow separates. The flow over the top of the cylinder shows a different behavior. For the unmodified cylinder the flow separates at the top leading edge and does not reattach. In the case of the cylinder with an elliptical afterbody, the flow detaches and reattaches on the top. The flow over the cylinder with a wedge in front does not show a separation. The amount of turbulent kinetic energy k, in each respective test case corresponds to the magnitude of its individual drag coefficient. The highest amount of turbulent kinetic energy and the largest coefficient of drag are observed for the flow around the unmodified cylinder.

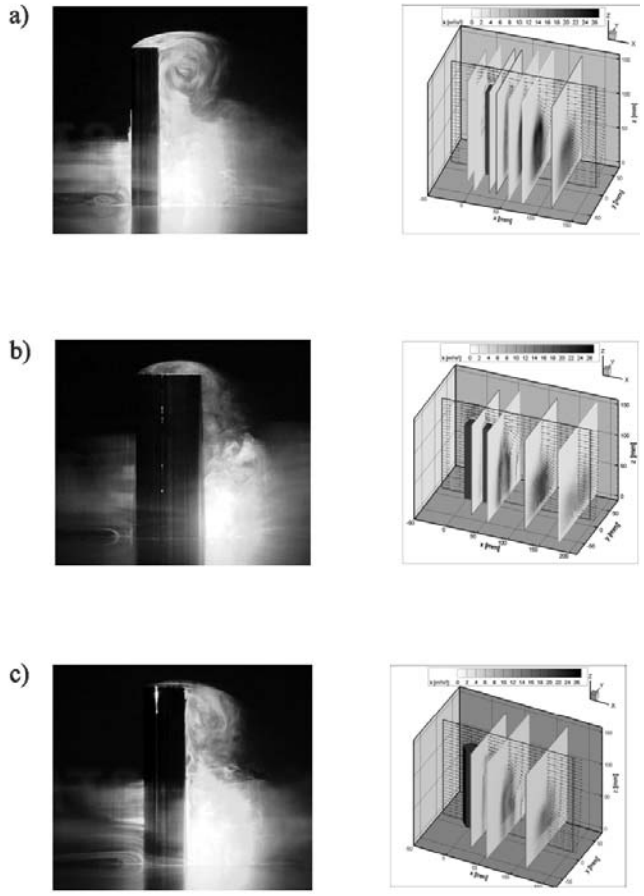

Figure 4: Flow visualization, velocity distribution and turbulent kinetic energy for a) unmodified cylinder, b) cylinder with elliptically afterbody and c) cylinder with wedge in front (U_0 = 10 m/s)

3 NUMERICAL SIMULATION

Two different unsteady fluid fields computed with the in-house CFD code FASTEST-3D developed and with the commercial CFD code ANSYS-CFX are used. In the simulation per-

formed with FASTEST-3D, LES (Large Eddy Simulation) using Smagorinsky model was applied to simulate the transient flow field with complete resolution of the boundary layer. Simulations were performed on SGI-ALTIX system with 16 processors using a numerical domain containing approximately 3.1 million volume cells and a time step size of $\Delta t = 10$ µs. For the simulation of the flow using the code ANSYS-CFX a turbulence modeling approach based on SAS (Scale Adaptive Simulation) was employed. The SAS approach allows to use coarser grids than those used in LES computations. Therefore approximately 1.1 million cells were used in this case, which resulted in a shorter computational time and less memory usage. Regarding time discretization, a time step size of $\Delta t = 20$ µs was used in this simulation.

Figure 5 shows the transient fluid fields obtained from both computations using Q factor analysis. The coherent structures are shown as iso-surface, for the values of $\lambda_{sym} = -10000$, where λ_{sym} is the eigenvalue of the symmetric tensor. The colour of the contour is based on the transient velocity.

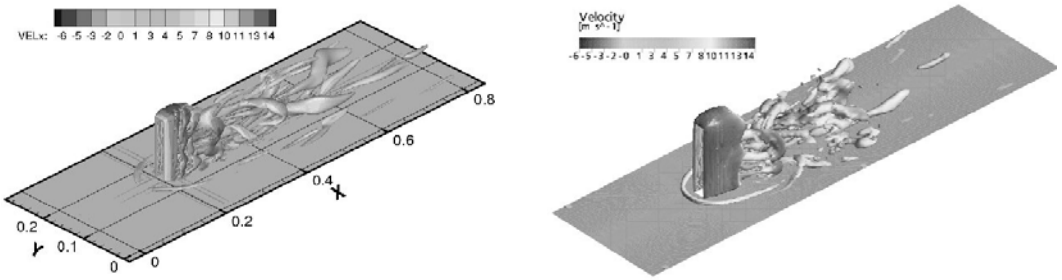

Fig.5 a) LES Simulation b) SAS - Simulation

4 COMPARISON

The direct comparison between the experimental and numerical results shows a good agreement in the mean flow velocities. The calculated turbulent kinetic energy is lower than what we obtained in the experiments. A stable vortex frequency cannot be identified. The flow behind the cylinder has a strong instationary character. There are different phase in the periodic vortex shedding, the classical Kármán type shedding breaks down to Arch type intermittently. The instationary flow is very complex and has a three-dimensional nature.

REFERENCES

[1] S. Becker, M. Kaltenbacher, I. Ali, C. Hahn, M. Escobar. Aeroacoustic Investigation of the Flow around Cylinder Geometries - a Benchmark Test Case, 13th AIAA/CEAS Aeroacoustics Conference, Rome, AIAA-2006-3511, 2007

[2] H. F. Wang. Flow structure around a finite-length square prism', 15th Australasian Fluid Mechanics Conference, University of Sydney, 13-17 September 2004.

[3] H. Sakamoto. Vortex shedding from a rectangular prism and a circular cylinder placed vertically in a turbulent boundary layer, *J. Fluid Mech.*, Vol. 126, pp. 147-165, 1983

[4] S. Becker, H. Lienhart, and F. Durst. Flow around three-dimensional obstacles in boundary layers, *J. Wind Eng.*, Vol. 90, pp. 265 --279, 2002.